Heliyon 10 (2024) e29516

Contents lists available at ScienceDirect

Heliyon

journal homepage: www.cell.com/heliyon

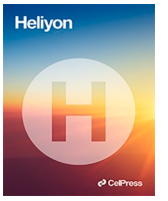

Research article

Preparation of VC nanoliposomes by high pressure homogenization: Process optimization and evaluation of efficacy, transdermal absorption, and stability

Yunqi Tang [a,b], Ankun Zhou [c], Shaodong Zhou [a,b], Jiancheng Ruan [a,b], Chao Qian [a,b,**], Chen Wu [a,b,*], Linlin Ye [c,***]

[a] College of Chemical and Biological Engineering, Zhejiang Provincial Key Laboratory of Advanced Chemical Engineering Manufacture Technology, Zhejiang University, Hangzhou, Zhejiang Province, 310027, PR China
[b] Institute of Zhejiang University-Quzhou, #99 Zheda Road, Quzhou, Zhejiang Province, 324000, PR China
[c] Hangzhou Yayan Cosmetics Co. Ltd., #9 Shunle Road, Hangzhou, Zhejiang Province, 311123, PR China

ARTICLE INFO

Keywords:
Vitamin C
Nanoliposomes
High-pressure homogenization
Skin permeation
Stability

ABSTRACT

Vitamin C (VC) possesses antioxidant and whitening effects. However, its effectiveness is hindered by challenges such as instability, impaired solubility, and limited bioavailability hinder. In this study, VC was encapsulated in nanoliposomes by primary emulsification and high-pressure homogenization. The VC nanoliposomes were comprehensively characterized for their microscopic morphology, particle size, polydispersity index (PDI), and encapsulation efficiency (EE). Orthogonal experiments were designed to optimize the optimal preparation process, and the antioxidant activity, whitening efficacy, transdermal absorption, and stability of VC nanoliposomes were evaluated based on this optimized process. The findings demonstrated the high reproducibility of the optimal process, with particle size, PDI, and EE values of 113.502 ± 4.360 nm, 0.104 ± 0.010, and 56.09 ± 1.01 %, respectively. Differential scanning calorimetry analysis showed effective encapsulation of VC nanoliposomes with better thermal stability than aqueous VC solution. Besides, the VC nanoliposomes demonstrated excellent antioxidant and whitening effects in efficacy experiments, stronger skin permeability in transdermal experiments and fluorescence tracking. Furthermore, storage stability tests indicated that the VC in nanoliposomes remained relatively stable after 60 days of storage. These findings highlighted the potential use of VC nanoliposomes in a wide range of applications for the cosmetic market, especially in the development of ingredients for skin care products.

1. Introduction

Vitamin C (VC), with the chemical formula $C_6H_8O_6$, is a polyhydroxy compound that easily dissolves in water. It is also known as L-ascorbic acid due to its acidic and strong reducing properties. VC plays a key role in collagen synthesis, mucopolysaccharide

* Corresponding author. College of Chemical and Biological Engineering, Zhejiang Provincial Key Laboratory of Advanced Chemical Engineering Manufacture Technology, Zhejiang University, Hangzhou, Zhejiang Province, 310027, PR China.
** Corresponding author. Institute of Zhejiang University-Quzhou, #99 Zheda Road, Quzhou, Zhejiang Province, 324000, PR China.
*** Corresponding author. Hangzhou Yayan Cosmetics Co. Ltd., #9 Shunle Road, Hangzhou, Zhejiang Province, 311123, PR China.
E-mail addresses: qianchao@zju.edu.cn (C. Qian), chenwu2333@zju.edu.cn (C. Wu), 54391919@qq.com (L. Ye).

https://doi.org/10.1016/j.heliyon.2024.e29516
Received 15 January 2024; Received in revised form 25 March 2024; Accepted 9 April 2024
Available online 10 April 2024

production, and can help reduce skin damage caused by free radicals, thus slowing down skin aging. Additionally, VC can inhibit the formation of abnormal skin pigments and tyrosinase activity, contributing to reduced melanin formation. As a result, it is widely used in skin whitening and antioxidant skincare cosmetics [1,2]. However, since VC is water-soluble, it has difficulty penetrating into the skin stratum corneum. Additionally, VC is susceptible to oxidation and unstable in water. To address these issues, VC is currently mainly available in solid tablets or used in the form of derivatives [3]. However, VC in its solid state is not efficiently absorbed by the body, and derivatives of VC often have reduced functionality due to significant increases in molecular weight and decreases in intramolecular VC. For example, magnesium ascorbyl phosphate is less effective than VC for its weak skin penetration, and ascorbyl 6-palmitate may lead to skin damage after UV exposure because of the formation of harmful free radical metabolites from its lipid molecules [3,4]. Therefore, it is crucial to explore approaches to improve the stability of VC and ensure its efficacy for various applications.

Liposomes have a cell-like membrane structure, with phospholipid bilayers capable of encapsulating hydrophilic, lipophilic, or amphiphilic active substances. They are widely utilized as delivery systems for active ingredients in cosmetics [5]. Liposomes not only demonstrate excellent skincare efficacy, but also serve as a protective shield for the encapsulated active ingredients, gradually releasing the active ingredients to minimize skin irritation. Furthermore, the unique structure of liposomes facilitates seamless integration with skin cells, promoting the transdermal absorption of active substances [6,7]. Nanoliposomes, possessing similar physical and thermodynamic properties to conventional liposomes, offer enhanced bioavailability of encapsulated active substances owing to their smaller particle size and higher surface-to-volume ratio [8], and hold great potential for cosmetic applications.

However, conventional methods for preparing nanoliposomes, such as thin-film dispersion [9], ethanol injection [10], and reversed-phase evaporation [11], suffer from the shortcomings of complex preparation processes, large liposome particle sizes, low encapsulation rates, and limited stability [12–14]. In addition, these methods often involve the use of irritating organic solvents and cholesterol, which may have adverse effects on the human body [15]. In recent years, high-pressure homogenization has been reported for the production of liposomes, which can avoid the use of a large number of irritating organic solvents in the traditional method, resulting in liposomes with small average particle sizes, uniform distribution, good stability, and suitable for large-scale production. This method involves emulsifying the oil and water phases and subsequently pressurizing them through microfine channels, using high pressure flow to generate significant shear, impact, and cavitation in order to obtain small-sized, uniformly distributed liposome suspensions [16,17].

Numerous reports have been published on the preparation of liposomes using the high-pressure homogenization method. Chung et al. [18] combined reverse phase evaporation and high-pressure homogenization to prepare cationic polymer-coated liposomes, and studied their physicochemical properties. Saroglu et al. [19] prepared saffron extract-loaded nanoliposomes (70 nm) encapsulated with chitosan of different molecular weights using the high-pressure homogenization method, which demonstrated high acid stability, slow-release properties, and protection of safranin under in vitro digestion conditions. However, there have been few reports on the production of VC nanoliposomes using high-pressure homogenization. Normally, these nanoliposomes are prepared using the traditional thin-film dispersion method or ethanol injection method [20,21], which is not suitable for mass production due to its limited dosage each time, time-consuming nature, and low efficiency. The utilization of high-pressure homogenization could significantly enhance the production efficiency, yielding liposomes with small particle sizes and uniform distributions, ideal for industrial application in cosmetics and food production.

In this study, we prepared VC nanoliposomes by employing a combination of primary emulsification and high-pressure homogenization techniques. To ensure the safety of human skin, we replaced irritating or toxic organic solvents with cosmetic-grade glycerin. Stable VC nanoliposomes were successfully obtained by carefully designing the water-oil ratio even without the use of cholesterol in the formulation. Moreover, orthogonal experiments were conducted to determine the optimal process parameters. The microscopic morphology, particle size, polydispersity index (PDI), and encapsulation efficiency of the VC nanoliposomes were comprehensively described. Furthermore, we investigated the antioxidant activity, whitening efficacy, transdermal absorption effect, and stability of the VC nanoliposomes under the optimized process conditions.

2. Materials and methods

2.1. Materials

Phospholipids were purchased from Simingshan Biotech (Ningbo, China). Vitamin C was provided by DSM Nutritional Products Ltd. (Shanghai, China). Glycerin was obtained from Procter & Gamble International Operations SA Singapore Branch (Shanghai, China). Caprylic/capric triglycerides (GTCC) were acquired from BASF SE (Shanghai, China). 2,2-Diphenyl-1-picrylhydrazyl (DPPH) was bought from Aladdin Biochemical Technology Co., Ltd. (Shanghai, China). 2,2'-Azinobis-(3-ethylbenzthiazoline-6-sulphonate) (ABTS) was purchased from Macklin Biochemical Technology Co., Ltd. (Shanghai, China). Ultra-purified water was used throughout the whole experimental process.

2.2. Rats skin

Male Sprague-Dawley rats weighing 200 ± 20 g were purchased from Huashu Biotechnology Co. (Hangzhou, China). Animal welfare and experimental procedures were strictly in accordance with the Guide for the Care and Use of Laboratory Animals and the related ethics regulations of Zhejiang University.

2.3. Nanoliposomes preparation

2.3.1. Initial emulsification

As depicted in Fig. 1, lecithin was dissolved in glycerin with a small amount of GTCC as a penetration enhancer, and stirred at 60 °C for 30 min 4 g of VC was dissolved in an aqueous citric acid solution (pH = 3.5) and stirred at 60 °C for 5 min. Subsequently, the oil and water phases were combined and stirred at 60 °C for 30 min to obtain VC liposome crude emulsion.

2.3.2. High pressure homogenization

The VC liposome crude emulsion was processed using a high-pressure homogenizer, with the pressure adjusted within a range of 480–920 bar. The homogenization process was cycled for 4–10 min to achieve the formation of VC nanoliposomes. The homogenizer valve is a key component of a high-pressure homogenizer. As depicted in Fig. 2, it consists of a pair of symmetrical slits that form a narrow channel. When high-speed fluid passes through the homogenizer valve, it is restricted by the slits, leading to significant shear and impact forces, causing collisions and friction between sample molecules and particles. The particles in the fluid undergo high-speed impact with the homogenizer valve, further promoting particle fragmentation. Rapid pressure changes result in the cavitation effect, which also leads to particle fragmentation. Through the combined effects of shear, impact, and cavitation, uniform sample particles with small size and enhanced stability could be achieved.

2.4. Optimization of preparation process of VC nanoliposomes

The prescription and preparation process of VC nanoliposomes were optimized by orthogonal experiments based on single-factor experiments. The microscopic morphology, particle size, PDI and encapsulation efficiency of liposomes were used as indicators, which was converted into a final score for comprehensive investigation. The main factors affecting liposomes were selected: lecithin concentration (A), glycerin content (B), homogenization time (C), and homogenization pressure (D).Each factor was taken at 3 levels. Thus, orthogonal L9 (3^4) experiments were performed and the detailed conditions for preparation of liposomes were shown in Table 1.

The overall rating was calculated as the cumulative value of all parameters examined (total score of 100), including microscopic morphology, particle size, PDI, and encapsulation efficiency. Each parameter was worth 25 % of the score.

2.5. Characterizations of VC loaded nanoliposomes

2.5.1. Morphology by transmission electron microscopy

The morphology of the prepared liposomes was determined by transmission electron microscope (TEM, HT-7700, HITACHI, Tokyo, Japan) with a negative staining method [22].

10 μL sample was pipetted onto a 300-mesh ultra-thin copper grid, allowed to dry naturally. And then it was negatively stained with a drop of 2 % phosphotungstic acid solution for 30 min. The excess liquid was blotted out with filter paper, dried and placed under a 120 kv TEM to examine its microscopic morphology.

2.5.2. Thermal analysis by differential scanning calorimetry

Differential scanning calorimetry (DSC) was utilized to check the thermal stability of fabricated nanoliposomes by using a

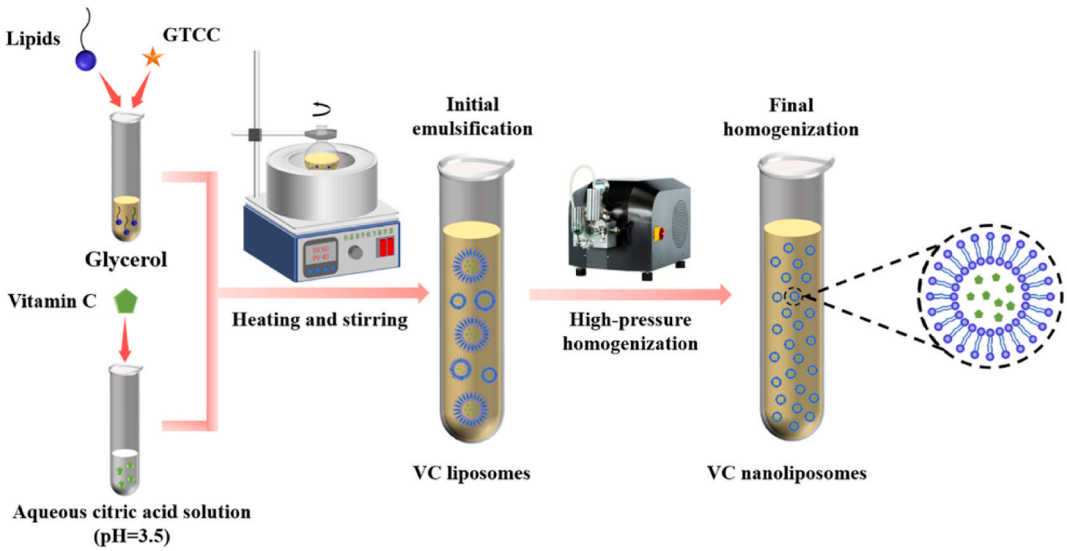

Fig. 1. Flow chart for the preparation of VC nanoliposomes.

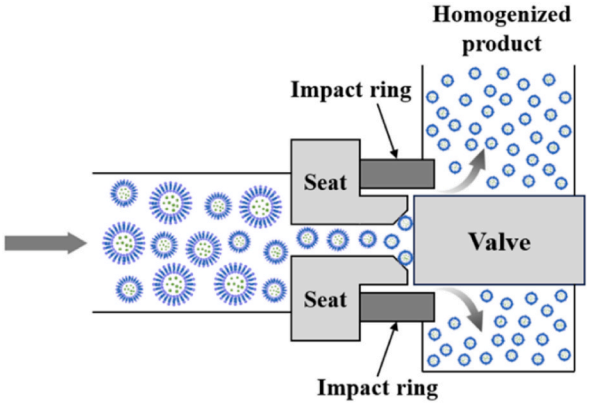

Fig. 2. Internal schematic structure of high-pressure homogenizer and homogenization process.

Table 1
Factors and levels for orthogonal experiments.

Level	Factor			
	A	B	C	D
	lecithin concentration (g/mL)	glycerol content (mL)	homogenization time (min)	homogenization pressure (bar)
1	0.100	15	4	500 ± 20
2	0.125	23	7	750 ± 20
3	0.150	30	10	900 ± 20

synchronous thermal analyzer (TGA/DSC 3+, Mettler, Switzerland). 15 mg sample was placed in hermetically sealed aluminum pans at a heating rate of 10 °C/min within a temperature range of 0–400 °C and under constant purging of nitrogen.

2.5.3. Particle size and size distribution

The average particle size and PDI of nanoliposomes were measured at 25 °C using dynamic light scattering (DLS) (Zetasizer Nano-ZS, Malvern, UK). The intensity was measured at a scattering angle of 90°. Samples (1 mL) were diluted 10-fold with ultra-purified water to prevent scattering phenomena.

2.5.4. Encapsulation efficiency

The encapsulation efficiency (EE) of VC was determined according to a slightly modified method described by Yang's group [23,24]. The free VC was separated from liposomes by dialysis. 1 mL of liposomal suspension was placed into a dialysis bag (3500 Da MW cut-off) and immersed in 1000 mL deionized water for 24 h with mild stirring, and the deionized water was refreshed every 2 h. Then, the VC content of the sample in the dialysis bag was quantified by UV–visible (UV–vis) spectrophotometry (UV-3500, Linchy LAB, Shanghai, China). In short, the pre- and post-dialysis liposomes were mixed with 2 mL methanol, respectively, and sonicated for 30 min to demulsify the composite liposomes. Then the mixture solution was placed into a 10 mL colorimetric tube followed by adding 0.3 mL of Na_2EDTA (0.25 M), 0.5 mL of acetic acid (0.5 M), and 1.25 mL of fast blue B salt (2 g/L) in sequence, then diluted to 10 mL with an aqueous citric acid solution. After thorough vortexing, the mixture was placed at ambient temperature for 30 min. The absorbance of the mixture was determined at 420 nm using a UV–vis spectrophotometer. The content of VC was calculated using a standard curve. Each experiment was carried out in triplicate.

The EE of VC (EE_{VC}) was calculated using Eq. (1):

$$EE_{VC}(\%) = \frac{W_{en}}{W_{total}} \times 100\% \quad (1)$$

Here, W_{total} and W_{en} are the amounts of VC in the liposomal suspension before and after dialysis, respectively.

2.5.5. Efficacy test

2.5.5.1. DPPH free radical scavenging capacity. The DPPH radical scavenging assay was determined according to the method reported by Dewi's group [25] with slight modifications. Aqueous VC solution, VC nanoliposomes obtained by optimized process, and blank liposomes were prepared at concentrations of 1, 5, 10, 15, and 20 μg/mL, respectively, as samples to be used. 1 mL of each sample was mixed with 1 mL of 0.2 mg/mL DPPH ethanol solution and 2 mL deionized water. The mixture was kept in the dark for 30 min, and then its absorbance was measured at 514 nm using a UV–vis spectrophotometer. The percentage of the DPPH-scavenging activity was

calculated using Eq. (2):

$$\text{DPPH radical activity}(\%) = \left(1 - \frac{T - T_0}{C - C_0}\right) \times 100\% \quad (2)$$

Here, T is the absorbance of 1 mL of samples, 1 mL of DPPH ethanol solution, and 2 mL deionized water. T_0 is the absorbance of 1 mL of samples, 1 mL of ethanol, and 2 mL deionized water. C is the absorbance of 1 mL of DPPH ethanol solution and 3 mL of ethanol. C_0 is the absorbance of 4 mL of ethanol.

2.5.5.2. ABTS free radical scavenging capacity. The ABTS radical scavenging assay was determined according to the method reported by Hosseini's group [26] with slight modifications. Aqueous VC solution, VC nanoliposomes obtained by optimized process, and blank liposomes were prepared at concentrations of 1, 5, 10, 15, and 20 μg/mL, respectively, as samples to be used. For the ABTS reserve solution, 10 mL of ABTS reserve solution (7.4 mM) was mixed with 10 mL of $K_2S_2O_8$ solution (2.6 mM), and the ABTS solution was obtained after 12 h–14 h at 4 °C in the dark. The ABTS solution was diluted to $A_{734} = 0.70 \pm 0.02$ before use. 100 μL of sample was added to 100 μL of ABTS solution. The mixture was placed in the dark for 30 min. The absorbance of the mixture was then measured at 734 nm using an enzyme marker (Spark, TECAN, Switzerland). Three replicate wells were set up for each concentration, and the above experiment was repeated three times. The percentage of the ABTS-scavenging activity was calculated using Eq (3):

$$\text{ABTS radical activity}(\%) = \left(1 - \frac{A_{\text{experimental}} - A_{\text{control}}}{A_{\text{standard}}}\right) \times 100\% \quad (3)$$

Here, $A_{\text{experimental}}$ is the absorbance of 100 μL of samples and 100 μL of ABTS. A_{control} is the absorbance of 100 μL of samples and 100 μL of ethanol. A_{standard} is the absorbance of 100 μL of deionized water and 100 μL of ethanol.

2.5.5.3. Tyrosinase inhibition capacity. The tyrosinase inhibition assay was determined according to the method reported by Gupta et al. [27] with slight modifications. Aqueous VC solution, VC nanoliposomes obtained by optimized process, and blank liposomes were prepared at concentrations of 50, 100, 150, 200, 250, and 300 μg/mL, respectively, as samples to be used. 1 mL of samples was mixed with 1 mL of 0.1 g/mL substrate L-tyrosine and 1 mL of phosphate buffer (pH = 6.8). After incubation at 37 °C for 10 min in the dark, 0.5 mL 100 U/mL tyrosinase solution was added to the mixture. The absorbance of each well was measured at 475 nm using a UV–vis spectrophotometer. The percentage of the tyrosinase inhibitory activity was calculated using Eq. (4):

$$\text{tyrosinase inhibitory}(\%) = \left(1 - \frac{A_1 - A_2}{A_3 - A_4}\right) \times 100\% \quad (4)$$

Here, A_1 is the absorbance of solution with active tyrosinase and sample. A_2 is the absorbance of solution with inactivated tyrosinase and sample. A_3 is the absorbance of solution with active tyrosinase and phosphate buffer. A_4 is the absorbance of solution with inactivated tyrosinase and phosphate buffer.

2.5.6. In vitro skin permeation study

In order to compare the skin permeation of VC from aqueous VC solution and VC nanoliposomes obtained by optimized process, a Franz diffusion cell method was employed [28,29] using a drug transdermal diffusion tester (RYJ-6B, Pharmaceutical Testing Instrument Co. Shanghai, China). The concentration of VC was 1500 μg/mL in all samples.

The rat skin was mounted onto Franz diffusion cell with diffusion areas of 2.2 cm^2. Each formulation (1.0 mL) was applied on the skin and allowed to spread evenly over the skin. The receptor compartment was filled with 6.4 mL of phosphate buffer (pH = 7.25), which was continuously stirred with a small magnetic rotor at 37.0 ± 0.5 °C. 0.5 mL of the sample was withdrawn periodically (1, 2, 3, 4, 5, 7, 9, 11, 14, 18, 24 and 48 h) from the receptor solution, and assayed by the UV–vis spectrometer. Meanwhile, the same volume of phosphate buffer was added to the receiver to maintain a constant volume. The cumulative infiltration per unit area was calculated using Eq. (5):

$$Q_n = \frac{C_n V + \sum_{i=1}^{n-1} C_i V_i}{A} \quad (5)$$

Here, C_n is the drug concentration in the receiving fluid at the nth sampling point (μg/mL); V is the volume of the receiving fluid in the receiving cell (6.4 mL); C_i is the drug concentration in the receiving fluid from the 1st to the last sampling (μg/mL); V_i is the sampling volume (0.5 mL); A is the effective skin permeation area (2.2 cm^2).

The transdermal rate Y_n was calculated using Eq. (6):

$$Y_n = \frac{Q_n A}{M} \times 100\% \quad (6)$$

Here, Q_n is the cumulative permeation per unit area of the nth sampling point (μg/cm^2); A is the effective skin permeation area (2.2 cm^2); M is the mass of VC in 1.0 mL sample (μg).

To investigate the permeation mechanism of VC in nanoliposomes through the skin in vitro, zero-order, first-order, Higuchi, and Korsmeyer-Peppas kinetic models (Eqs. (7)-(10)) were utilized for analysis [30]:

Zero-order model: $M_t/M_\infty = kt$ (7)

First-order model: $M_t/M_\infty = 1\text{-}e^{-kt}$ (8)

Higuchi model: $M_t/M_\infty = kt^{1/2}$ (9)

Korsmeyr-Peppas model: $M_t/M_\infty = kt^n$ (10)

Here, M_t is the cumulative penetration of the active ingredient at time t, M_∞ is the theoretical maximum cumulative penetration of the active ingredient, and k is a kinetic constant. In the Korsmeyr-Peppas model, n is the release index, which can be used to characterize the release mechanism. The correlation coefficients (R^2) of the above four kinetic modeling equations were obtained by fitting to determine whether the in vitro transdermal absorption conformed to the drug release pattern.

2.5.7. Confocal laser scanning microscopy (CLSM) study

To monitor the localization of VC liposomes for transdermal administration, we labeled the liposomes with fluorescein diacetate (FDA) and applied them to a rat skin model. Similarly, the fluorescent FDA-loaded nanoliposomes were prepared using the same method, with the exception of using FDA instead of VC in step 2.3. Additionally, the same concentration of FDA solution (0.48 mM) was prepared with DMSO as the solvent and used as as a control.

The rat skin was mounted onto Franz diffusion cell with diffusion areas of 2.2 cm^2. 0.5 mL of each formulation was applied and allowed to spread over the skin. The receptor compartment was filled with 6.4 mL of phosphate buffer (pH = 7.25), which was continuously stirred with a small magnetic bar at 37.0 ± 0.5 °C.

The rat skin was removed immediately after 13 h of transdermal treatment and sent to frozen section. In other words, the skin was embedded with embedding agent in the longitudinal direction and cut into several thin slices of rat skin with a thickness of 7 μm. The thin slices of rat skin were carried on slides and subsequently examined for fluorescence using a laser confocal microscope (CLSM, A1, Nikon, Tokyo, Japan) at an excitation wavelength of 488 nm and an emission wavelength of 525 nm.

2.5.8. Stability study

The nanoliposomes stability was studied over a period of 60 days by investigating different changes in particles size, PDI, and EE. They were stored in the dark at 25 °C, with aliquots withdrawn for analysis on days 7, 14, 21, 28, 35, 42, 49, and 60. The changes in the appearance of the nanoliposomes were also photographed and recorded. Particle size and PDI were determined by DLS as described in section 2.5.3. The EE during storage was calculated as stated in section 2.5.4.

Table 2
The result of orthogonal experiment. Data are presented as means ± SD (n = 3), different lowercase letters indicate significant differences between groups ($P < 0.05$).

Formula	A lecithin concentration (g/mL)	B glycerol content (mL)	C homogenization time (min)	D homogenization pressure (bar)	Microscopic morphology	Size (nm)	PDI	EE_{VC}	Overall rating
1	1	1	1	1	Fig. 2A	173.367 ± 1.466^{i}	0.136 ± 0.027^{cd}	32.69 ± 1.01%^{e}	55
2	1	2	2	2	Fig. 2B	226.467 ± 1.466^{g}	0.045 ± 0.039^{e}	41.01 ± 1.03%^{c}	65
3	1	3	3	3	Fig. 2C	382.467 ± 3.792^{d}	0.095 ± 0.013^{de}	48.91 ± 2.02%^{b}	72
4	2	1	2	3	Fig. 2D	260.800 ± 0.356^{f}	0.187 ± 0.016^{bc}	55.77 ± 1.00%^{a}	59
5	2	2	3	1	Fig. 2E	340.167 ± 1.586^{e}	0.153 ± 0.039^{c}	53.11 ± 3.01%^{ab}	75
6	2	3	1	2	Fig. 2F	488.400 ± 3.254^{b}	0.146 ± 0.013^{cd}	34.91 ± 1.02%^{de}	35
7	3	1	3	2	Fig. 2G	208.767 ± 0.946^{h}	0.234 ± 0.008^{ab}	50.10 ± 2.00%^{b}	50
8	3	2	1	3	Fig. 2H	716.933 ± 8.298^{a}	0.215 ± 0.025^{ab}	42.27 ± 0.92%^{c}	29
9	3	3	2	1	Fig. 2I	441.433 ± 3.357^{c}	0.246 ± 0.021^{a}	38.91 ± 1.01%^{cd}	36
K_1	192	164	119	166					
K_2	169	169	160	150					
K_3	115	143	197	160					
$K_1/3$	64.00	54.67	39.67	55.33					
$K_2/3$	56.33	56.33	53.33	50.00					
$K_3/3$	38.33	47.67	65.67	53.33					
R	25.67	8.67	26.00	5.33					

2.5.9. Statistical analysis

The data were expressed as the mean values ± standard deviation (SD, n = 3 independent samples) and the results were analyzed statistically for significance ($p < 0.05$) using SPSS 18.0 software (IBM Corp., Armonk, NY, USA). Origin 9.0 (OriginLab Inc., Northampton, MA, USA) was used to draw graphs.

3. Results and discussion

3.1. Optimal preparation process of VC nanoliposomes

As indicated in Table 2, the parameters investigated in this study included lecithin concentration (A), glycerol content (B), homogenization time (C), and homogenization pressure (D). Groups of nine orthogonal groups set according to these four parameters showed significant differences in particle size, PDI and EE ($p < 0.05$). Homogenization time represents the number of cycles and directly affects the particle size and dispersion. Merima et al. [31] found that as the number of cycles increases, the size of liposomes decreases and the PDI value decreases. However, beyond five cycles, there was no significant reduction in liposome size or PDI value; in fact, the PDI value slightly increased, potential due to the vesicle re-growth as a result of particle aggregation and instability. Moreover, lecithin concentration determines the moldability of liposomes and the degree of encapsulation. Guldiken et al. [32] had suggested that more extracts could be encapsulated in liposomes containing higher lecithin concentrations. However, Sebaaly et al. [33] found that too high lecithin concentration increased the particle size and PDI value of liposomes. Glycerol content affects the particle size and permeability of liposomes. Abdellatif et al. [34] found that the presence of high concentrations of glycerol led to alterations in the fluidity of the lipid bilayer membranes, which in turn reduced the size of the vesicles and allowed more drug to penetrate into the skin. Furthermore, the effect of the homogenizing pressure on particle size is non-linear. Increasing the pressure reduces the particle size, but excessive pressure may cause the liposomes breakage, reaggregation, and fluctuations in particle size. Chen et al. [35] showed that the particle size of curcumin liposomes varied from 150.0 nm to 200.0 nm at the working pressures of 100 MPa and 200 MPa. However, as the operating pressure increased from 300 MPa to 400 MPa, the particle size of curcumin liposomes

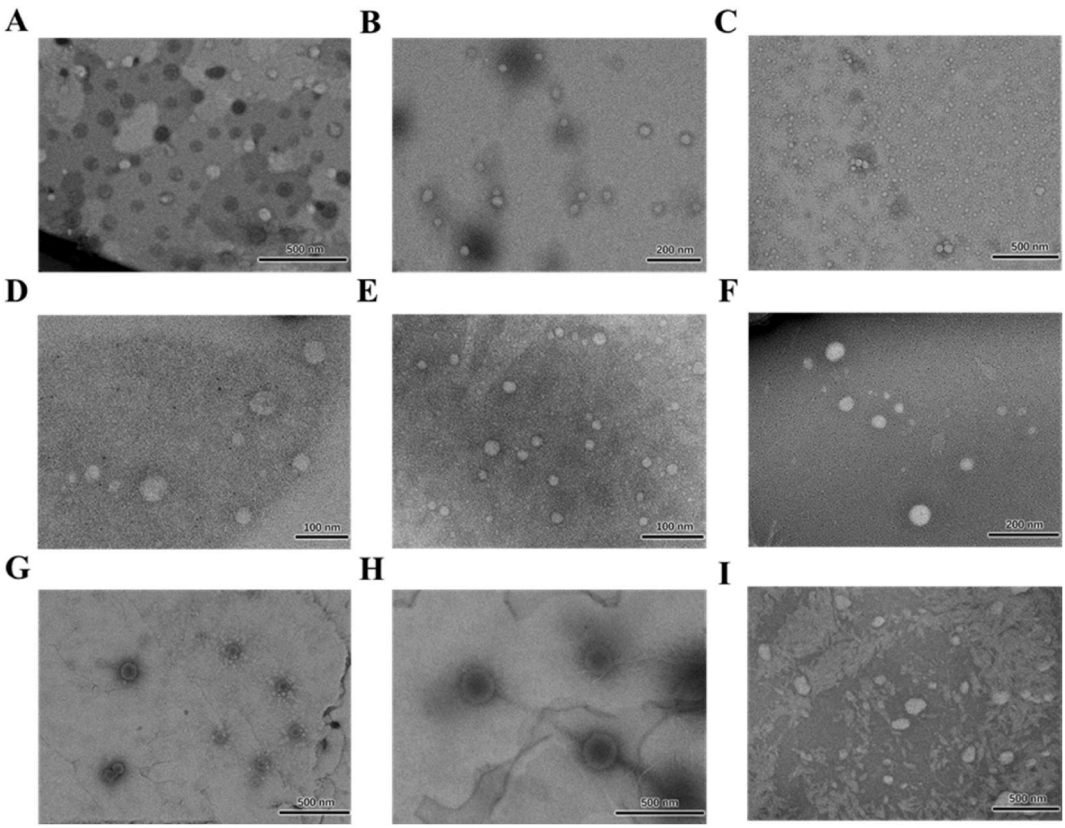

Fig. 3. TEM images showing the morphologies of nanoliposomes in different orthogonal groups. (A: lecithin concentration 0.100 g/mL, glycerol content 15 mL, homogenization time 4 min, homogenization pressure 500 ± 20 bar; B: 0.100 g/mL, 23 mL, 7 min, 750 ± 20 bar; C: 0.100 g/mL, 30 mL, 10 min, 900 ± 20 bar; D: 0.125 g/mL, 15 mL, 7 min, 900 ± 20 bar; E: 0.125 g/mL, 23 mL, 10 min, 500 ± 20 bar; F: 0.125 g/mL, 30 mL, 4 min, 750 ± 20 bar; G: 0.150 g/mL, 15 mL, 10 min, 750 ± 20 bar; H: 0.150 g/mL, 23 mL, 4 min, 900 ± 20 bar; I: 0.150 g/mL, 30 mL, 7 min, 500 ± 20 bar)

increased, which was attributed to the fact that the higher operating pressure over-compressed the curcumin liposomes, resulting in the aggregation of samples. Therefore, instead of discussing variable experiments for a single factor, this study conducted orthogonal experiments based on different factors to explore the interrelationships between the factors and to strike a proper balance between all the key parameters.

As indicated in Fig. 3 and Table 2, the ranges of lecithin concentration, glycerol content, homogenization time, and homogenization pressure were 24.00, 9.67, 25.67, and 4.67, respectively. The larger the range, the greater the impact. Based on the range values, the priority of the four factors could be ranked in the following order: C > A > B > D. Therefore, in this study system, homogenization time was the first factor affecting the formation of VC nanoliposomes, followed by lecithin concentration, glycerol content ranked third, and homogenization pressure ranked the last.

3.2. Optimal process repeated results

The optimal condition determined based on the microscopic morphology, particle size, PDI, and EE was found to be A_1 B_2 C_3 D_1. Therefore, the optimal formulation of VC nanoliposomes consisted of a lecithin concentration of 0.1 g/mL, glycerin content of 23 mL, homogenization time of 10 min, and homogenization pressure of 500 ± 20 bar. To validate the optimization results, we replicated the process and prepared three batches of VC nanoliposomes. The average values of particle size, PDI, and EE were found to be 113.502 ± 4.360 nm, 0.104 ± 0.010, and 56.09 ± 1.01 %, respectively. EE is a critical indicator of liposome performance, reflecting the extent to which the active ingredient is encapsulated within the carrier. Factors such as the liposome's composition, its preparation method, and the bilayer's physical rigidity exert significant impacts on the active ingredient's EE. Generally, liposomes exhibit limited encapsulation capacity for water-soluble drugs, with an encapsulation rate exceeding 50 % deemed satisfactory [13]. This EE surpassed that of VC nanoliposomes reported by Hassane Hamadou et al. [36] (52.09 %), Yang et al. [24] (47.16 %), and Lv et al. [37] (53.49 %). As shown in Fig. 4, the majority of the prepared nanoliposomes exhibited a uniform spherical shape without any noticeable breakage or agglomeration. Taking into consideration the results of all parameters, the overall mean rating for liposomes in the three groups was 82, the highest among all the orthogonal groups. Therefore, we can conclude that the selected formulation and preparation process were stable, feasible, and highly reproducible.

3.3. Thermal behavior analysis

As shown in Fig. 5, at low temperature ranges, three weak endothermic peaks were observed for the blank liposomes at 88 °C, 133 °C, and 140 °C, indicating a phase transition from the gel state to the liquid crystalline state. Similar phenomena were also observed in the DSC assay for the nanoliposomes prepared by Xu's group, but they only had two heat absorption peaks and low temperatures, which were related to the source of lecithin and the proportion of cholesterol added [30]. After encapsulation, only one peak at 87 °C was observed at a similar location, possibly indicating an increase in the intercalation of the phospholipid acyl chains with GTCC and glycerol, which allowed the nanoliposomes to be compacted by reducing the mobility of the molecular chains [38,39]. Both blank liposomes and VC nanoliposomes showed a small peak at 86–88 °C, which could be considered a characteristic peak for liposomes. Additionally, the aqueous VC solution exhibited a peak at 107 °C, whereas VC nanoliposomes and blank liposomes showed no peak at this temperature. The absence of the endothermic peak in nanoliposomes suggested interactions between VC and liposomes hinders the decomposition of VC, confirming the successful encapsulation of VC [40]. At higher temperatures, all three samples showed pronounced heat absorption peaks, with the aqueous VC solution at 189 °C, VC nanoliposomes at 238 °C, and blank liposomes at 253 °C, representing their respective melting temperatures. Moreover, the phase transition temperature of VC nanoliposomes was comparable to that of blank liposomes and significantly higher than that of the aqueous VC solution, indicating improved thermal stability after VC encapsulated into the liposomes. The more pronounced peak of VC nanoliposomes suggested a more ordered arrangement in the bilayer membrane [41]. These results confirmed the successful encapsulation of VC nanoliposomes, and the enhanced thermal stability of VC nanoliposomes compared with the aqueous VC solution.

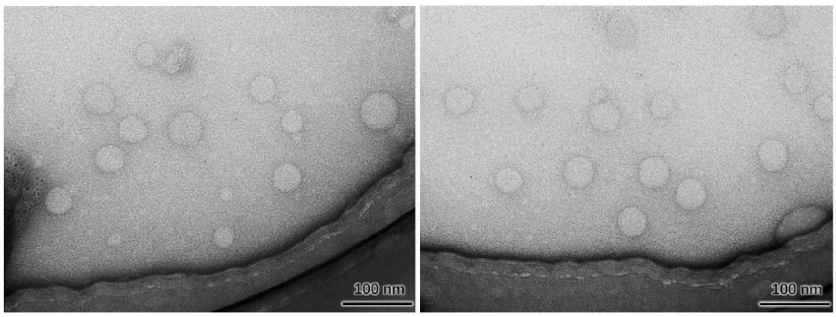

Fig. 4. TEM images showing the morphologies of optimal nanoliposomes.

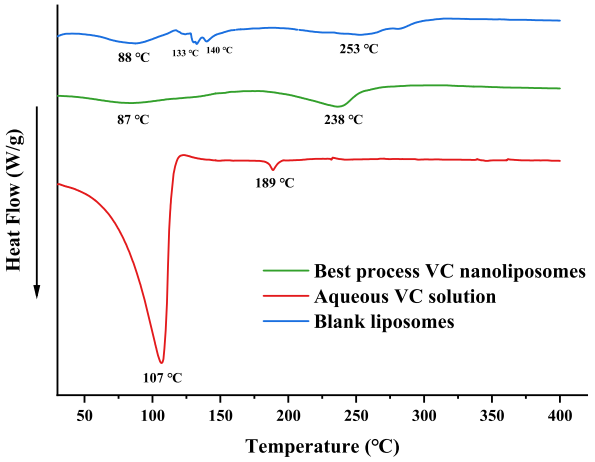

Fig. 5. Thermal behavior of aqueous VC solution, VC nanoliposomes, and blank liposomes determined by DSC.

3.4. DPPH radical activity

VC, when used in cosmetics, offers numerous benefits such as the elimination of oxygen free radicals, improved skin repair and regeneration, as well as a deceleration of the aging process. To evaluate the in vitro antioxidant capacity of VC-loaded nanoliposomes, the DPPH test was employed, as oxidative stress is a major contributor to skin roughness and discoloration. As depicted in Fig. 6A, initially, the elimination rate of the aqueous VC solution (12.69 %) was slightly higher than that of VC nanoliposomes (12.60 %). However, at a VC concentration of 5 μg/mL, the elimination rates were similar, and the rate of VC nanoliposomes (22.44 %) was marginally higher than that of the aqueous VC solution (22.01 %). Notably, when the concentration exceeded 5 μg/mL, the elimination rate of VC nanoliposomes significantly surpassed that of the aqueous VC solution, with the elimination rate increasing along with concentration enhancement. It was also observed that the blank liposomes demonstrated some level of antioxidant activity. This could be attributed to the antioxidant properties of lecithin, which could directly scavenge free radicals. The unsaturated hydrocarbon chains and phosphate groups of the phospholipids in lecithin can be a hydrogen atom donor and electron acceptor to bind with free radicals and exert antioxidant effects [42]. This suggested that the combined effect of lecithin and VC enhanced the antioxidant capacity of VC nanoliposomes. Moreover, previous studies have shown that nano-formulations of VC exhibited heightened antioxidant activity compared to free VC [43], further confirming that the clearance of VC nanoliposomes at higher concentrations was superior to that of aqueous VC solution. This holds great significance for the antioxidant efficacy of cosmetics.

3.5. ABTS radical activity

The ABTS radical activity test, similar to the DPPH test, is commonly used to evaluate antioxidant activity. However, the ABTS test specifically examines the water-soluble free radical scavenging ability, while the DPPH test assesses the lipid-soluble ability.

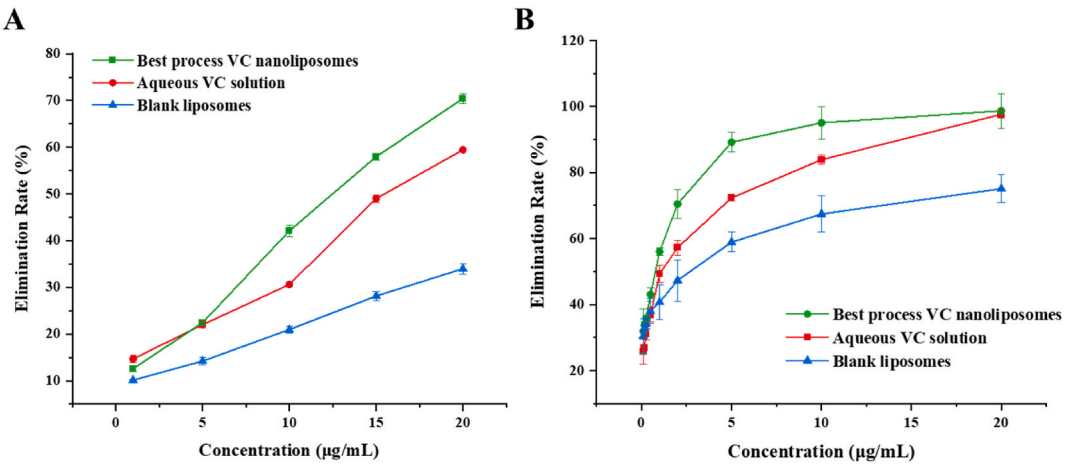

Fig. 6. DPPH (A) and ABTS (B) radical elimination rate of aqueous VC solution, VC nanoliposomes, and blank liposomes. Data are presented as means ± SD (n = 3).

Additionally, the ABTS test is used to measure the activity of hydrogen donor compounds and/or chain-breaking antioxidants [26,44]. As illustrated in Fig. 6B, the elimination rate of both aqueous VC solution and VC nanoliposomes increased with increasing concentration, but the elimination rate of VC nanoliposomes was superior to the aqueous VC solution. At a concentration of 20 μg/mL, both removal rates were close to each other, however, the elimination rate of VC nanoliposomes (98.70 %) was still slightly higher than that of aqueous VC solution (97.64 %). Moreover, the blank liposomes also exhibited some ABTS radical scavenging ability. This further underscored the fact that the combined effect of VC and lecithin enhanced the scavenging ability of VC nanoliposomes. The results of the ABTS assay showed a similar trend to those of the DPPH assay, indicating the potential for the development of cosmetics with enhanced antioxidant properties.

3.6. Tyrosinase inhibitory activity

Melanin, culprit for skin pigmentation, is produced in the body through the catalysis of tyrosinase from tyrosine to intermediary compounds like dopa pigments. VC can effectively reduce and inhibit melanin production by suppressing tyrosinase activity and reducing dopa pigment formation. This leads to a whitening effect by reducing the appearance of spots [45]. We conducted a tyrosinase inhibition experiment to evaluate the whitening performance of VC nanoliposomes. As depicted in Fig. 7A, the results demonstrated that the anti-tyrosinase activity increased with increasing concentration of the tested extract. At concentrations below 150 μg/mL, the inhibition rate of VC nanoliposomes surpassed that of the aqueous VC solution. However, at a concentration of 200 μg/mL, the inhibition rate of the aqueous VC solution (45.65 %) started to exceed that of VC nanoliposomes (41.05 %). At a concentration of 300 μg/mL, the tyrosinase inhibition effect of the aqueous VC solution (88.89 %) was better than that of VC nanoliposomes (72.58 %). This may be due to the fact that the encapsulation of liposomes affected the release at high VC concentrations, and the slow release of VC resulted in a slightly lower rate of inhibition than aqueous VC solution. A similar situation has been reported in the literature [46,47]. In conclusion, it can be concluded that VC encapsulated by lecithin was able to maintain its biological activity. The inhibitory effect of VC nanoliposomes on tyrosinase was similar to that of the aqueous VC solution at low concentrations, and showed a slow-release effect at high concentrations. Additionally, the negligible tyrosinase inhibition observed with blank liposomes indicated that the whitening effect of VC nanoliposomes was primarily attributed to VC itself.

3.7. In vitro skin permeation study

In vitro skin penetration studies were conducted on rat skin to evaluate the penetration of VC encapsulated in liposomal formulations. As indicated in Fig. 7B, during the initial 5-h period, the penetration rate of VC exhibited a rapid increase. Subsequently, between 5 and 18 h, the penetration rate of the aqueous VC solution decelerated, with the cumulative penetration amount being markedly lower compared to VC nanoliposomes. From 18 to 48 h, the rate of permeation gradually slowed down in both groups, but the amount of VC permeation was still increasing. The cumulative amounts of permeated VC after 48 h were ranked as follows: VC nanoliposomes (422.33 ± 15.64 μg/cm^2) > aqueous VC solution (277.83 ± 12.38 μg/cm^2). This clearly indicated that VC nanoliposomes exhibited better efficacy in penetration. Additionally, the transdermal rate of VC nanoliposomes (61.94 %) was significantly higher than that of aqueous VC solution (40.75 %). These results further confirmed that the cell-like membrane structure of liposomes allowed for better fusion with the skin, facilitating the penetration of encapsulated VC into the skin [48]. Moreover, some studies have shown that nanoscale liposomes have superior permeation effects compared to regular liposomes [24]. They conducted transdermal experiments comparing VC nanoliposomes and regular liposomes, and found that VC nanoliposomes exhibited better sustainable release of the drug and higher skin penetration compared to VC liposomes. In a study by Schramlová [49], the skin permeation of

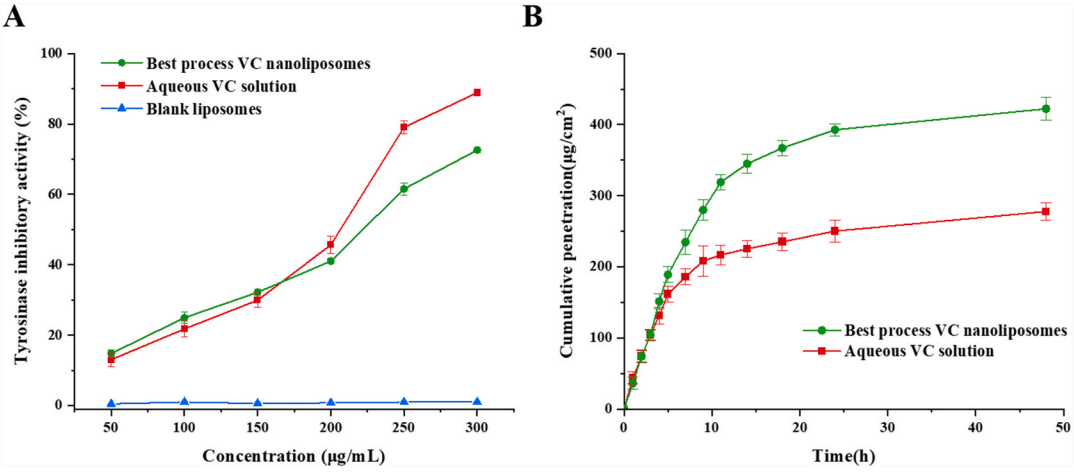

Fig. 7. Tyrosinase inhibitory rate (A) and skin permeation profiles (B) of aqueous VC solution and VC nanoliposomes. Data are presented as means ± SD (n = 3).

protein G-gold conjugate liposomes was investigated and it was observed that the smaller the particle size, the better the transdermal effect of the liposomes. These reports strongly supported the findings of our present experiments.

To better understand the transdermal mechanism of bioactive compounds, in vitro transdermal data was analyzed using four different kinetic equations. The cumulative permeation rate of VC in *in vitro* skin permeation was fitted to the zero-order model, first-order model, Higuchi model and Korsmeyer-Peppas model, respectively. The kinetic equations and parameters for the permeation of VC from VC nanoliposomes and aqueous VC solution were presented in Table 3. During the initial 18 h, the permeation amounts of VC nanoliposomes and aqueous VC solution were well-fitted to the zero-order model. From 0 to 48 h, the best fit to the first-order model was obtained, with R^2 values of 0.9943 for VC nanoliposomes and 0.9847 for aqueous VC solution. This indicated that the in vitro transdermal absorption test data were reliable and consistent with a first-order kinetic model of drug release, and the results were similar to those already reported in the literature [50,51]. Furthermore, the value of n in the Korsmeyer-Peppas model can be used to explain the release mechanism of the actives. n values of 0.421 and 0.335 in the Korsmeyer-Peppas fitting equations for VC nanoliposomes and aqueous VC solution, respectively, were less than 0.45, suggesting that the permeation of the active ingredient was primarily driven by Fickian diffusion, and the active ingredient VC within VC nanoliposomes primarily permeated through molecular diffusion across the phospholipid bilayer of the liposomes [51,52].

3.8. CLSM study

CLSM can be utilized to visualize the distribution of fluorescent probes during the skin permeation process. To further analyze and compare the skin penetration ability and distribution of VC nanoliposomes and aqueous VC solution, a 13-h transdermal experiment was conducted using homo-systemic nanoliposomes encapsulating FDA fluorescein. A control group was prepared with the same concentration of FDA solution (0.48 mM) using DMSO as the solvent. The CLSM images in Fig. 8 were depicted as longitudinal cross-section of rat skin from both sets of transdermal experiments. The nanoliposome group exhibited abundant green fluorescence in both the stratum corneum and the dermis, while the aqueous group only showed fluorescence within the stratum corneum. This suggested that the nanoliposomes facilitated the penetration of the encapsulated drug, allowing it to reach deeper layers of the skin. Furthermore, we observed strong fluorescence signals in the hair follicles of the skin samples treated with nanoliposomes at specific time intervals. This implied that a significant amount of fluorescein may accumulate in the hair follicles and penetrated deeper into the skin through these follicles.

Zhang et al. [53] developed a core-shell structured Lecithins-Zein nanoparticles (KLZ-NPs) loaded with ketoconazole. Through the CLSM, they visualized the dynamic transport processes of coumarin-6 nanoparticles in the skin to simulate KLZ-NPs. Their findings indicated that KLZ-NPs could enhance the penetration of the loaded drug into the skin by utilizing skin attachment structures such as hair follicles, thereby increasing drug retention in the skin. In a separate study conducted by Tanha's group [54], alcohol plasma was employed to encapsulate hyaluronic acid, and rhodamine B was also incorporated into the system (with a particle size of 100 nm). CLSM results demonstrated that cumulative skin penetration increased over an 8-h period, indicating that the nano-systems were capable of penetrating into the dermis. Additionally, Verma et al. [55] showed that liposomes with a smaller diameter of 120 nm exhibited significantly enhanced penetration of CF (a hydrophilic fluorescent compound) in the skin compared to larger liposomes. This suggested that nanoliposomes can effectively regulate the depot effect of hydrophilic drugs in the skin, with smaller particle sizes leading to better permeation effects. These findings supported the scientific validity of our experiments and illustrate that VC nanoliposomes, with their extremely small particle size (around 100 nm), can effectively penetrate into the dermis by utilizing skin attachment structures like hair follicles. Such insights were valuable for delivering hydrophilic active substances into deeper layers of the skin and enabling them to exert their skincare functions.

3.9. Storage stability study

For the development of cosmetics, it is important not only to have a specific efficacy, but also to have a certain long-term stability. Liposomes encapsulating active substances can encounter storage-related challenges, such as phospholipid hydrolysis and decomposition of the encapsulated drug [56]. These chemical degradation processes may be due to the hydrolysis of ester bonds connecting the fatty acids to the glycerin backbone and the peroxidation of unsaturated acyl chains [57]. Additionally, excessive particle size and

Table 3
Model fitness of VC cumulative release from liposomal formations in vitro skin permeation.

Sample	Model	Time Period (h)	Fitting Equation	R^2	Transdermal Rate
VC nanoliposomes	Zero order model	0–18	$M_t/M_\infty = 0.0296t + 0.0895$	0.9012	53.86 %
	Zero order model	0–48	$M_t/M_\infty = 0.0117t + 0.2143$	0.6117	61.94 %
	First order model	0–48	$M_t/M_\infty = 0.6251(1\text{-}e^{-0.1138t})$	0.9943	61.94 %
	Higuchi model	0–48	$M_t/M_\infty = 0.1059t^{1/2} + 0.0285$	0.8378	61.94 %
	Korsmeyer-Peppas model	0–48	$M_t/M_\infty = 0.1423t^{0.4215}$	0.8610	61.94 %
Aqueous VC solution	Zero order model	0–18	$M_t/M_\infty = 0.0160t + 0.1142$	0.7905	34.50 %
	Zero order model	0–48	$M_t/M_\infty = 0.0064t + 0.1809$	0.5723	40.75%
	First order model	0–48	$M_t/M_\infty = 0.3788(1\text{-}e^{-0.1762t})$	0.9847	40.75 %
	Higuchi model	0–48	$M_t/M_\infty = 0.0584t^{1/2} + 0.0778$	0.8029	40.75 %
	Korsmeyer-Peppas model	0–48	$M_t/M_\infty = 0.1260t^{0.3348}$	0.8681	40.75 %

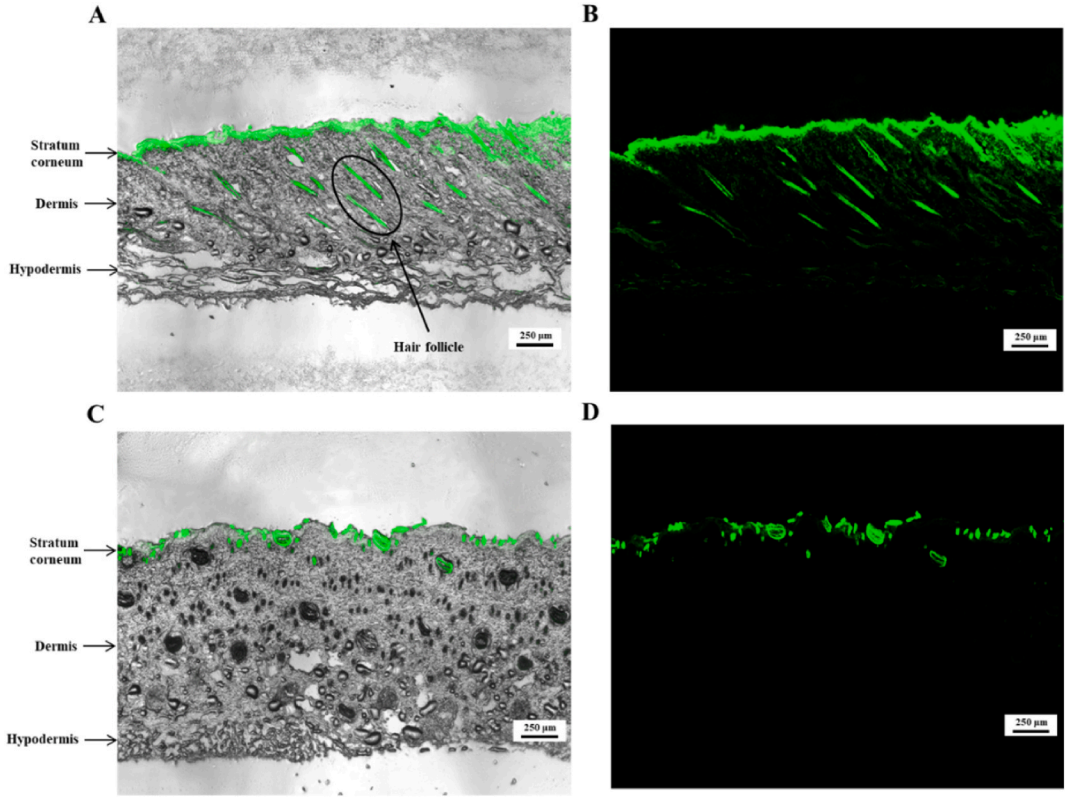

Fig. 8. (A) and (B) Images of the combination of FDA nanoliposomes in bright field and fluorescence. (C) and (D) Images of the combination of FDA solution in bright field and fluorescence.

size distribution can lead to liposome settling or aggregation [58]. Therefore, it is essential to investigate the stability of liposomes.

As depicted in Fig. 9A, following a 60-day storage period at 25 °C, the nanoliposomes exhibited a darkening surface color, suggesting a potential slight oxidation of free VC. However, no presence of flocculent material or delamination was observed, indicating the stability advantage of the nanoliposomes. As shown in Fig. 9B, the particle size of the nanoliposomes experienced minimal changes throughout the entire 60-day storage period at 25 °C, with a modest increase of approximately 1.24-fold (from 113.5 to 140.2 nm). The PDI values gradually increased over the storage period (from 0.104 to 0.144), but they remained below 0.3 throughout the 60-day storage period. The EE of VC nanoliposomes exhibited a decreasing trend over time, which could be attributed to the chemical degradation of phospholipids and changes in the fluidity of the liposome membranes during storage. This may result in membrane disruption and fusion, allowing the active ingredients loaded in the aqueous cores to gradually leak out of the liposomes [59,60]. However, the EE of VC nanoliposomes decreased by only 8.77 % (from 56.09 % to 47.32 %) within 60 days, suggesting that the nanoliposomes provided a relatively stable barrier for the encapsulated VC. The changes in these three parameters were consistent with existing reported results [36].

In summary, VC nanoliposomes demonstrated relative stability across various parameters over a 60-day storage period. The enhanced stability of liposome-encapsulated VC can be attributed to the molecular-level interaction between VC and the phospholipid bilayer [61]. Additionally, the bilayers provided protective effects against liposome decomposition and served as a shield on the liposome's surface [62]. Furthermore, the high-pressure homogenization treatment ensured the VC nanoliposomes maintained a small particle size and a well-dispersed state, contributing to the overall system's stability. Therefore, it can be concluded that liposome encapsulation techniques significantly improved the stability of VC, and the high-pressure homogenization treatment played a crucial role in enhancing the storage stability of the nanoliposomes.

4. Conclusion

In this study, we prepared VC nanoliposomes using a combination of primary emulsification and high-pressure homogenization, avoiding the use of irritating or toxic organic solvents. The optimal preparation process was determined through orthogonal experiments. The results indicated that the nanoliposomes prepared using this process exhibited optimal microscopic morphology, particle size, PDI, EE, and were reproducible. The antioxidant properties of VC nanoliposomes prepared by the optimal process were superior to the aqueous VC solution. Moreover, the whitening efficacy was comparable to that of aqueous VC solution, with improved propermeation functions observed in transdermal experiments. CLSM study revealed that the active substances in nanoliposomes

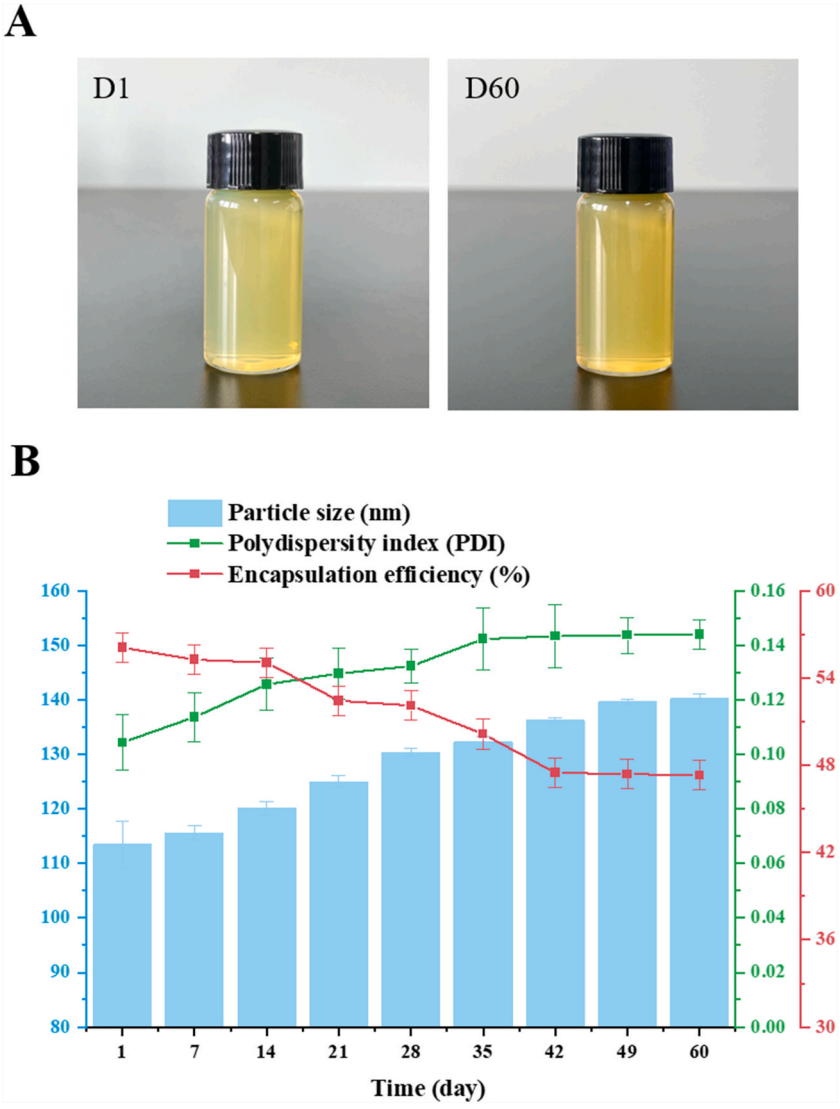

Fig. 9. Physical appearance (A) and stability study (B) of nanoliposomes over 60-day storage period at 25 °C. Data are presented as means ± SD (n = 3).

penetrated deeper layers of skin by accumulating in the hair follicles. Furthermore, VC nanoliposomes displayed improved thermal and storage stability.

This study has significant implications in two aspects. Firstly, it contributes to enhancing the storage stability of VC. Secondly, it offers a fast and gentle process for nanoliposome preparation, which can serve as a valuable reference for designing efficient delivery systems for hydrophilic active substances. As a result, it holds significant practical importance for product development in the food and cosmetics industries, especially in the development of active ingredients for efficacy-oriented skincare products.

Funding statement

Generous financial support by the *Key Research and Development Program of Zhejiang Province, China* (2023C01102, 2023C01208, 2022C01208).

Data availability

Data will be made available on request.

CRediT authorship contribution statement

Yunqi Tang: Writing – original draft, Investigation. **Ankun Zhou:** Visualization, Investigation. **Shaodong Zhou:** Software, Conceptualization. **Jiancheng Ruan:** Validation, Data curation. **Chao Qian:** Methodology, Conceptualization. **Chen Wu:** Writing – review & editing. **Linlin Ye:** Supervision, Methodology.

Declaration of competing interest

Authors declare that there is no conflict of interest

Acknowledgement

The authors thank for the Zhejiang Xin'an Chemical Industrial Group Co., Ltd. for employing Professor Chao Qian as the Specially-appointed expert of the Qianjiang Talents Program in Hangzhou City.

References

[1] J. Du, J.J. Cullen, G.R. Buettner, Ascorbic acid: chemistry, biology and the treatment of cancer, Biochim. Biophys. Acta 1826 (2012) 443–457.
[2] A.N. Zaid, R. Al Ramahi, Depigmentation and anti-aging treatment by natural molecules, Curr. Pharmaceut. Des. 25 (2019) 2292–2312.
[3] C.D. Enescu, L.M. Bedford, G. Potts, F. Fahs, A review of topical vitamin C derivatives and their efficacy, J. Cosmet. Dermatol. 21 (2022) 2349–2359.
[4] N.P. Stamford, Stability, transdermal penetration, and cutaneous effects of ascorbic acid and its derivatives, J. Cosmet. Dermatol. 11 (2012) 310–317.
[5] S. Shah, V. Dhawan, R. Holm, M.S. Nagarsenker, Y. Perrie, Liposomes: advancements and innovation in the manufacturing process, Adv. Drug Deliv. Rev. 154–155 (2020) 102–122.
[6] S.I. Park, E.O. Lee, H.M. Yang, C.W. Park, J.D. Kim, Polymer-hybridized liposomes of poly(amino acid) derivatives as transepidermal carriers, Colloids Surf. B Biointerfaces 110 (2013) 333–338.
[7] W. Liu, W.L. Liu, C.M. Liu, J.H. Liu, S.B. Yang, H.J. Zheng, H.W. Lei, R. Ruan, T. Li, Z.C. Tu, X.Y. Song, Medium-chain fatty acid nanoliposomes for easy energy supply, Nutrition 27 (2011) 700–706.
[8] E. Acosta, Bioavailability of nanoparticles in nutrient and nutraceutical delivery, Curr. Opin. Colloid Interface Sci. 14 (2009) 3–15.
[9] S. Amiri, M. Rezazadeh-Bari, M. Alizadeh-Khaledabad, S. Amiri, New formulation of vitamin C encapsulation by nanoliposomes: production and evaluation of particle size, stability and control release, Food Sci. Biotechnol. 28 (2019) 423–432.
[10] X. Liu, P. Wang, Y.X. Zou, Z.G. Luo, T.M. Tamer, Co-encapsulation of Vitamin C and beta-Carotene in liposomes: storage stability, antioxidant activity, and in vitro gastrointestinal digestion, Food Res. Int. 136 (2020) 109587.
[11] Y. Li, G. Jia, T. Li, X. Zhou, H. Zhao, J. Cao, Z. Guan, R. Zhao, Preparation optimization and immunological activity studies of portulaca oleracea L. Polysaccharides liposomes, Curr. Pharmaceut. Des. 30 (2024).
[12] V. Van Tran, J.-Y. Moon, Y.-C. Lee, Liposomes for delivery of antioxidants in cosmeceuticals: challenges and development strategies, J. Contr. Release 300 (2019) 114–140.
[13] M.A. Chaves, L.S. Ferreira, L. Baldino, S.C. Pinho, E. Reverchon, Current applications of liposomes for the delivery of vitamins: a systematic review, Nanomaterials 13 (2023).
[14] T. Peng, W. Xu, Q. Li, Y. Ding, Y. Huang, Pharmaceutical liposomal delivery—specific considerations of innovation and challenges, Biomater. Sci. 11 (2023) 62–75.
[15] X. Su, D. Peng, The exchangeable apolipoproteins in lipid metabolism and obesity, Clin. Chim. Acta 503 (2020) 128–135.
[16] M. Stang, H. Schuchmann, H. Schubert, Emulsification in High-Pressure Homogenizers, vol. 1, Engineering in Life Sciences, 2001.
[17] S. Schultz, G. Wagner, K. Urban, J. Ulrich, High-pressure homogenization as a process for emulsion formation, Chem. Eng. Technol. 27 (2004) 361–368.
[18] S.K. Chung, G.H. Shin, M.K. Jung, I.C. Hwang, H.J. Park, Factors influencing the physicochemical characteristics of cationic polymer-coated liposomes prepared by high-pressure homogenization, Colloids Surf. A Physicochem. Eng. Asp. 454 (2014) 8–15.
[19] O. Saroglu, B. Atalı, R.M. Yıldırım, A. Karadag, Characterization of nanoliposomes loaded with saffron extract: in vitro digestion and release of crocin, J. Food Meas. Char. 16 (2022) 4402–4415.
[20] R. Wang, C. Ma, H. Yan, H. Zhao, P. Wang, S. Zhang, J. Ju, S. Yu, Z. Yin, Lecithin/cholesterol/tween 80 liposomes for Co-encapsulation of vitamin C and xanthoxylin, ACS Appl. Nano Mater. 7 (2024) 5982–5995.
[21] A. Khuntia, R. Kumar, Y. Premjit, J. Mitra, Release behavior of vitamin C nanoliposomes from starch–vitamin C active packaging films, J. Food Process. Eng. 45 (2022) e14075.
[22] Z. Jiao, X. Wang, Z. Chen, Folate-conjugated methoxy poly (ethylene glycol)/poly (L-Alanine) amphiphilic block copolymeric micelles for targeted delivery of paclitaxel, Drug Deliv. 18 (2011) 478–484.
[23] W. Chen, M. Zou, X. Ma, R. Lv, T. Ding, D. Liu, Co-encapsulation of EGCG and quercetin in liposomes for optimum antioxidant activity, J. Food Sci. 84 (2019) 111–120.
[24] S. Yang, W. Liu, C. Liu, W. Liu, G. Tong, H. Zheng, W. Zhou, Characterization and bioavailability of vitamin C nanoliposomes prepared by film evaporation-dynamic high pressure microfluidization, J. Dispersion Sci. Technol. 33 (2012) 1608–1614.
[25] I.K. Dewi, Indarto Suhendriyo, S. Pramono, A. Rohman, R. Martien, Total phenolic and flavonoid content, free radical scavenging activity and tyrosinase inhibition of corn cob (zea mays) extract, Int. J. Appl. Pharm. (2021) 99–102.
[26] S.F. Hosseini, L. Ramezanzade, M. Nikkhah, Nano-liposomal entrapment of bioactive peptidic fraction from fish gelatin hydrolysate, Int. J. Biol. Macromol. 105 (2017) 1455–1463.
[27] S.D. Gupta, S.K. Masakapalli, Mushroom tyrosinase inhibition activity of Aloe vera L. gel from different germplasms, Chin. J. Nat. Med. 11 (2013) 616–620.
[28] S. Shanmugam, C.K. Song, S. Nagayya-Sriraman, R. Baskaran, C.S. Yong, H.G. Choi, D.D. Kim, J.S. Woo, B.K. Yoo, Physicochemical characterization and skin permeation of liposome formulations containing clindamycin phosphate, Arch Pharm. Res. (Seoul) 32 (2009) 1067–1075.
[29] K.H. Kang, Y.W. Choi, Influence of liposome type and skin model on skin permeation and accumulation properties of genistein, J. Dispersion Sci. Technol. 31 (2010) 1061–1066.
[30] T. Xu, J. Zhang, R. Jin, R. Cheng, X. Wang, C. Yuan, C. Gan, Physicochemical properties, antioxidant activities and in vitro sustained release behaviour of co-encapsulated liposomes as vehicle for vitamin E and beta-carotene, J. Sci. Food Agric. 102 (2022) 5759–5767.
[31] M. Ibišević, A. Smajlović, I. Arsić, Optimization of high pressure homogenization in the production of liposomal dispersions, Technologica Acta 12 (2020) 7–10.
[32] B. Guldiken, M. Gibis, D. Boyacioglu, E. Capanoglu, J. Weiss, Physical and chemical stability of anthocyanin-rich black carrot extract-loaded liposomes during storage, Food Res. Int. 108 (2018) 491–497.
[33] C. Sebaaly, H. Greige-Gerges, S. Stainmesse, H. Fessi, C. Charcosset, Effect of composition, hydrogenation of phospholipids and lyophilization on the characteristics of eugenol-loaded liposomes prepared by ethanol injection method, Food Biosci. 15 (2016) 1–10.

[34] M.M. Abdellatif, I.A. Khalil, M.A.F. Khalil, Sertaconazole nitrate loaded nanovesicular systems for targeting skin fungal infection: in-vitro, ex-vivo and in-vivo evaluation, Int. J. Pharm. 527 (2017) 1–11.
[35] W.-T. Chen, H.-T. Wu, I.C. Chang, H.-W. Chen, W.-P. Fang, Preparation of curcumin-loaded liposome with high bioavailability by a novel method of high pressure processing, Chem. Phys. Lipids 244 (2022) 105191.
[36] A. Hassane Hamadou, W.-C. Huang, C. Xue, X. Mao, Formulation of vitamin C encapsulation in marine phospholipids nanoliposomes: characterization and stability evaluation during long term storage, LWT - Food Sci. Technol. 127 (2020) 109439.
[37] X. Lv, Z. Wu, X. Qi, High skin permeation, deposition and whitening activity achieved by xanthan gum string vitamin c flexible liposomes for external application, Int. J. Pharm. 628 (2022) 122290.
[38] A.M. Liao, B. Cai, J.H. Huang, M. Hui, K.K. Lee, K.Y. Lee, C. Chun, Synthesis, anticancer activity and potential application of diosgenin modified cancer chemotherapeutic agent cytarabine, Food Chem. Toxicol. 148 (2021) 111920.
[39] V. Campani, L. Scotti, T. Silvestri, M. Biondi, G. De Rosa, Skin permeation and thermodynamic features of curcumin-loaded liposomes, J. Mater. Sci. Mater. Med. 31 (2020) 18.
[40] C.U. Istenic, Natasa Poklar, Encapsulation of (-)-epigallocatechin gallate into liposomes and into alginate or chitosan microparticles reinforced with liposomes, J. Sci. Food Agric. 96 (2016).
[41] J. Huang, M. Wu, K. Yang, M. Zhao, D. Wu, J. Ma, B. Ding, W. Sun, Effect of nanoliposomal entrapment on antioxidative hydrolysates from goose blood protein, J. Food Sci. 85 (2020) 3034–3042.
[42] O. Koprivnjak, D. Škevin, S. Valić, V. Majetić, S. Petričević, I. Ljubenkov, The antioxidant capacity and oxidative stability of virgin olive oil enriched with phospholipids, Food Chem. 111 (2008) 121–126.
[43] E. Parhizkar, M. Rashedinia, M. Karimi, S. Alipour, Design and development of vitamin C-encapsulated proliposome with improved in-vitro and ex-vivo antioxidant efficacy, J. Microencapsul. (2018) 1–11.
[44] M.E. Nasab, N. Takzaree, P.M. Saffaria, A. Partoazar, In vitro antioxidant activity and in vivo wound-healing effect of lecithin liposomes: a comparative study, J. Comparative Effectiveness Res. 8 (2019).
[45] U. Panich, V. Tangsupa-a-nan, T. Onkoksoong, K. Kongtaphan, K. Kasetsinsombat, P. Akarasereenont, A. Wongkajornsilp, Inhibition of UVA-mediated melanogenesis by ascorbic acid through modulation of antioxidant defense and nitric oxide system, Arch Pharm. Res. (Seoul) 34 (2011) 811–820.
[46] H.T. Kim, J. Lee, Y.J. Jo, M.J. Choi, Application of liposome encapsulating lactobacillus curvatus extract in cosmetic emulsion lotion, Materials 14 (2021).
[47] P. Ravikumar, M. Katariya, S. Patil, P. Tatke, R. Pillai, Skin delivery of resveratrol encapsulated lipidic formulation for melanoma chemoprevention, J. Microencapsul. 36 (2019) 535–551.
[48] G. Cevc, U. Vierl, Nanotechnology and the transdermal route: a state of the art review and critical appraisal, J. Contr. Release 141 (2010) 277–299.
[49] J. Schramlová, K. Blazek, M. Bartácková, B. Otová, D. Hulínská, Electron microscopic demonstration of the penetration of liposomes through skin, Folia Biol. 43 (1997) 165.
[50] K. Tai, M. Rappolt, X. He, Y. Wei, S. Zhu, J. Zhang, L. Mao, Y. Gao, F. Yuan, Effect of β-sitosterol on the curcumin-loaded liposomes: vesicle characteristics, physicochemical stability, in vitro release and bioavailability, Food Chemistry 293 (2019) 92–102.
[51] X. Xiao, X. Wu, Z. Yu, J. He, Incorporation of the sterol from camellia oil deodorant distillate into vitamin C liposomes: vesicle characteristics, stability, release, and bioavailability, Food Biophys. 18 (2023) 10–22.
[52] A. Jain, S.K. Jain, In vitro release kinetics model fitting of liposomes: an insight, Chem. Phys. Lipids 201 (2016) 28–40.
[53] S. Zhang, W. Song, H. Wu, J. Wang, Y. Wang, Z. Zhang, H. Lv, Lecithins-Zein nanoparticles for antifungal treatment: enhancement and prolongation of drug retention in skin with reduced toxicity, Int. J. Pharm. 590 (2020) 119894.
[54] A. Tanha, M. Rabiee, A. Rostami, S. Ahmadi, A green-based approach for noninvasive skin rejuvenation: potential application of hyaluronic acid, Environ. Res. (2023) 116467.
[55] D.D. Verma, S. Verma, G. Blume, A. Fahr, Particle size of liposomes influences dermal delivery of substances into skin, Int. J. Pharm. 258 (2003) 141–151.
[56] M.-K. Lee, L. Choi, M.-H. Kim, C.-K. Kim, Pharmacokinetics and organ distribution of cyclosporin A incorporated in liposomes and mixed micelles, Int. J. Pharm. 191 (1999) 87–93.
[57] B. Heurtault, P. Saulnier, B. Pech, J.E. Proust, J.P. Benoit, Physico-chemical stability of colloidal lipid particles, Biomaterials 24 (2003) 4283–4300.
[58] P.R. Karn, W. Cho, H.J. Park, J.S. Park, S.J. Hwang, Characterization and stability studies of a novel liposomal cyclosporin A prepared using the supercritical fluid method: comparison with the modified conventional Bangham method, Int. J. Nanomed. 8 (2013) 365–377.
[59] L. Pan, S. Zhang, K. Gu, N. Zhang, Preparation of astaxanthin-loaded liposomes: characterization, storage stability and antioxidant activity, CyTA - J. Food 16 (2018) 607–618.
[60] R. Huang, H. Song, X. Wang, H. Shen, S. Li, X. Guan, Fatty acids-modified liposomes for encapsulation of bioactive peptides: fabrication, characterization, storage stability and in vitro release, Food Chem. 440 (2024) 138139.
[61] C.J. Kirby, C.J. Whittle, N. Rigby, D.T. Coxon, B.A. Law, Stabilization of ascorbic-acid by microencapsulation in liposomes, Int. J. Food Sci. Technol. 26 (1991) 437–449.
[62] S. Bochicchio, A.A. Barba, G. Grassi, G. Lamberti, Vitamin delivery: carriers based on nanoliposomes produced via ultrasonic irradiation, LWT - Food Sci. Technol. 69 (2016) 9–16.